Scientific Research Publishing

Food and Nutrition Sciences, 2025, 16(9), 1097-1118
https://www.scirp.org/journal/fns
ISSN Online: 2157-9458
ISSN Print: 2157-944X

Proanthocyanidins-Rich *Euterpe oleracea* Mart Seed Extract Prevents Vascular and Perivascular Adipose Tissue Remodeling by Regulating the Renin-Angiotensin System, Inflammation, and Oxidative Damage in Diet-Induced Obese Mice

Matheus Henrique Romão[1], Graziele Freitas de Bem[1], Amanda Faria de Medeiros[1], Izabelle Barcellos Santos[1], Dafne Lopes Bessera Silva[1], Ricardo de Andrade Soares[2], Beatriz Cardoso de Oliveira[1], Dayane Teixeira Ognibene[1], Cristiane Aguiar da Costa[1], Ângela Castro Resende[1]*

[1]Department of Pharmacology, Institute of Biology, Rio de Janeiro State University, Rio de Janeiro, Brazil
[2]Institute of Biomedical Sciences, Federal University of Rio de Janeiro, Rio de Janeiro, Brazil
Email: *Angelaresende.uerj@gmail.com

How to cite this paper: Romão, M.H., de Bem, G.F., de Medeiros, A.F., Santos, I.B., Silva, D.L.B., de Andrade Soares, R., de Oliveira, B.C., Ognibene, D.T., da Costa, C.A. and Resende, Â.C. (2025) Proanthocyanidins-Rich *Euterpe oleracea* Mart Seed Extract Prevents Vascular and Perivascular Adipose Tissue Remodeling by Regulating the Renin-Angiotensin System, Inflammation, and Oxidative Damage in Diet-Induced Obese Mice. *Food and Nutrition Sciences*, **16**, 1097-1118.
https://doi.org/10.4236/fns.2025.169063

Received: August 7, 2025
Accepted: September 14, 2025
Published: September 17, 2025

Copyright © 2025 by author(s) and Scientific Research Publishing Inc.
This work is licensed under the Creative Commons Attribution International License (CC BY 4.0).
http://creativecommons.org/licenses/by/4.0/

Open Access

Abstract

Ectopic excessive fat deposition, including the perivascular adipose tissue (PVAT), may negatively influence vascular homeostasis and has emerged as a target for treating obesity-related vascular disease. The açaí (*Euterpe oleracea* Mart) seed extract (ASE) has beneficial metabolic effects, which could reduce the risk of obesity-related vascular disease. Therefore, this study aimed to investigate the impact of treatment with ASE on aorta remodeling and hypertension and evaluate its underlying mechanisms in a mouse model of obesity induced by a high-fat (HF) diet. Male C57BL/6 mice were divided into the groups: Control, HF, and HF + ASE (300 mg/kg/day for 12 weeks). We evaluated the systolic and diastolic blood pressure, PVAT, and aorta morphology and fibrosis parameters. Renin-angiotensin system (RAS) proteins, oxidative stress, and inflammatory biomarkers were evaluated in the aorta and PVAT by Western blotting and/or immunohistochemistry. ASE impaired weight gain, hypertension, PVAT hypertrophy and aorta morphological changes (media thickness, media-to-lumen ratio, and circumferential wall tension). ASE prevented the fibrosis by mitigating the increased deposition of type I collagen and TGF-β. The increased RAS components in the aorta (renin, AT1R) and PVAT (AT1R), as well as the decreased ACE2/ACE (aorta) and

AT2R (PVAT), were prevented by ASE. The overexpression of oxidative damage markers (NOX4 and 8-isoprostane) and pro-inflammatory cytokines (IL-6, TNF-α, and MCP-1) was impaired by ASE. The study indicates that ASE protects HF-fed mice from hypertension, PVAT and vascular wall remodeling by regulating PVAT and aortic RAS, as well as oxidative stress and inflammation.

Keywords

Açaí, Proanthocyanidins, Obesity, Vascular Remodeling, Perivascular Adipose Tissue

1. Introduction

Obesity rates are rising at an alarming pace both in Brazil and globally, contributing significantly to the growing number of cardiovascular disease (CVD) cases [1]-[3]. Poor dietary habits along with physical inactivity are key contributors to CVD associated with obesity, which in turn increases the risk of illness and death among affected individuals [4]-[6].

Obesity contributes to vascular remodeling, a process triggered by mechanical and hemodynamic changes, marked by increased arterial stiffness and thickening of the vascular media. This remodeling involves key features such as fibrosis and the proliferation of vascular smooth muscle cells (VSMCs) [7] [8]. Both experimental and epidemiological evidence indicate that arterial stiffness in individuals with obesity serves as a sign of vascular dysfunction and acts as an independent risk factor in the onset and progression of cardiovascular disease (CVD) [4] [9] [10]. Despite the potential benefits, few anti-obesity drugs have demonstrated favorable cardiovascular effects, with many showing limited effectiveness and raising concerns about safety [11]. This highlights a pressing need for the development of new therapeutic strategies targeting both obesity and its associated cardiovascular complications.

In this context, medicinal plants and natural compounds are considered safer alternatives due to their generally lower incidence of side effects. *Euterpe oleracea* Mart, commonly known as açaí, is a palm tree native to the Amazonian region. While its purple pulp is widely consumed in Brazil and exported to other countries, the seeds of açaí remain largely underutilized and overlooked. Interestingly, an extract obtained from açaí seeds (ASE) has been found to contain a higher concentration of polyphenols than the fruit Pulp [12]. This extract is rich in flavonoids, particularly proanthocyanidins, and exhibits significant biological activities, including vasodilatory, antioxidant, and anti-inflammatory effects [13]-[15]. Recent studies have shown that ASE can influence the local renin-angiotensin system (RAS) in the liver and white adipose tissue of mice fed a high-fat diet (HFD) [16] [17]. This modulation of the RAS may play a role in the positive effects of ASE on obesity-related conditions.

Obesity-related arterial remodeling and dysfunction are driven by several mechanisms, including alterations in the extracellular matrix (ECM), dedifferentiation of vascular smooth muscle cells (VSMCs), and impairments in both endothelial function and perivascular adipose tissue (PVAT) [9] [18]-[21]. PVAT is a metabolically active tissue that contributes significantly to vascular homeostasis by releasing various signaling molecules that facilitate paracrine communication with the vascular wall [15] [16]. In obesity, the secretory behavior of PVAT is altered, characterized by increased oxidative stress, inflammation, and disruptions in the RAS, which collectively contribute to reduced vascular relaxation and increased arterial stiffness [15] [17]. Considering its key involvement in the development of vascular diseases, PVAT represents a promising therapeutic target for innovative cardiovascular treatments [16] [17]. To date, there is no evidence demonstrating that ASE has a beneficial impact on PVAT as a therapeutic target for cardiovascular disease and obesity-related vascular wall changes.

Thus, this study sought to assess the potential protective effects of ASE, which is abundant in oligomeric and polymeric condensed tannins called proanthocyanidins, on vascular hypertrophy, fibrosis, and PVAT remodeling induced by a HFD in C57BL/6 mice. The mechanisms behind ASE's effects were studied by examining components of the RAS, oxidative stress, and inflammation in both the aorta and PVAT, as well as exploring potential interactions between these two tissues.

2. Materials and Methods

2.1. Preparation of Açaí Seed Extract (ASE)

Fruits of *Euterpe oleracea* Mart. were sourced from the Amazon Bay (Pará State, Brazil). The plant was authenticated at the Goeldi Museum (Belém do Pará, Brazil), where a voucher specimen was deposited under number MG 205222. The hydroalcoholic extract was prepared following the method previously established by our research group [13]. The pulp was first separated from the seeds, and 200 g of seeds were weighed. The seeds were boiled in 400 mL of water for 5 minutes. After boiling, 400 mL of ethanol was added to the mixture. The extract was then stored in a dark bottle at refrigerated temperature and shaken for 2 hours daily over a period of 10 days. Following this, the mixture was filtered using Whatman No. 1 filter paper, and the ethanol was removed by evaporation under reduced pressure at 55˚C. The remaining extract was freeze-dried at temperatures between −30˚C and −40˚C under a vacuum of 200 mmHg. Finally, the dried extract was kept at room temperature for future use.

Our group previously analyzed the aqueous residue fraction of ASE using high-performance liquid chromatography (HPLC) and MALDI-TOF mass spectrometry [22]. The HPLC results indicated that ASE is primarily composed of oligomeric and polymeric condensed tannins-proanthocyanidins ranging from monomers to decamers, which accounted for 88% of the total chromatographic area—along with minor quantities of catechin and epicatechin. The MALDI-TOF MS analysis identified two primary B-type proanthocyanidin peak series. The first series corresponded

to procyanidins ranging from trimers to undecamers [22]. The second series indicated heteropolymerization, featuring incorporation of (epi)gallocatechin units within the trimer to undecamer range. Additionally, 3-O-galloylated compounds were detected, including monogalloylated trimers, as well as mono-, di-, and trigalloylated tetramers and pentamers [22]. Therefore, chemical and spectrometric studies demonstrated that ASE mainly consists of polymeric procyanidins, heteropolymers containing a single gallocatechin unit, and a minor fraction of galloylated procyanidins [22].

2.2. Animals and Diet

Animal care and experimental protocols adhered to the regulations of the Brazilian Ministry of Science, Technology, and Innovation, in accordance with the National Council for the Control of Animal Experimentation (CONCEA/MCTI N˚ 49/2021). The study protocol received approval from the Animal Care and Use Committee (CEUA) at the Biology Institute of Rio de Janeiro State University (protocol number CEUA N˚ 002/2020, approved on 28/01/2020). All procedures complied with the NIH Guide for the Care and Use of Laboratory Animals as well as the ARRIVE 2.0 guidelines for reporting *in vivo* research.

Male C57BL/6 mice (n = 45), aged four weeks, were purchased from ANILAB (São Paulo). After one-week of acclimatization and at five weeks of age, the animals were housed in a controlled environment room with a 12-hour light/dark cycle (lights on at 6:00 a.m.), temperature maintained at 23˚C ± 2˚C, and relative humidity of 55% ± 5%. Food and water were provided ad libitum. The animals were randomly assigned to three groups (n = 15 per group): the control group received a standard diet (10% energy from lipids, 76% from carbohydrates, and 14% from proteins); the HF group was fed with an HFD (60% energy from lipids, 26% from carbohydrate and 14% from proteins) and HF + ASE group received the same HFD along with ASE treatment at a dose of 300 mg/kg/day administered orally by gavage for 12 weeks. The control and HF groups received only the vehicle (water) through oral gavage. The 12-week duration and ASE dosage for chronic treatment were selected based on prior research demonstrating the timeframe required to induce metabolic changes in C57BL/6 mice on a high-fat diet, as well as the effectiveness of ASE in improving metabolic disorders [22] [23]. The diets (detailed in the supplementary material) were formulated by Rhoster (São Paulo, Brazil) in accordance with the American Institute of Nutrition's (AIN-93M) guidelines for rodent maintenance and as previously reported [22].

The treatment allocation was performed by an independent researcher not involved in data collection, ensuring allocation concealment. The outcome assessment was conducted by assessors blinded to group assignments, and data analysis was performed using anonymized datasets, with analysts blinded to treatment allocation.

2.3. Body Weight and Glucose Measurements

Body weight was recorded weekly using a digital scale with a precision of 0.01 g, and

the average weight for each group was calculated throughout the 12-week treatment period. Blood glucose was measured before (initial glucose) and at the end of treatment following a 6-hour fasting period, using a glucometer (Accu-Chek Active; Roche, Mannheim, Germany).

2.4. Arterial Pressure Measurement

Systolic blood pressure was monitored weekly in conscious mice throughout the treatment period using caudal artery plethysmography. Measurements were taken with the CODA non-invasive blood pressure system for rodents (Kent Scientific Corp, Torrington, CT, USA). For each time point, the average of three consecutive readings was calculated (n = 15 per group).

2.5. Euthanasia and Tissue Extraction

At the end of the treatment period, mice were anesthetized via intraperitoneal injection of thiopental sodium (70 mg/kg). Blood was then collected by cardiac puncture from a coronary artery branch leading into the right ventricle. Plasma was isolated by centrifugation at 18,000 × g for 10 minutes at 4˚C and stored individually at −80˚C for subsequent analyses. The thoracic aorta was carefully dissected and immediately fixed, along with the thoracic aorta TAPV, in a solution of formalin (1.27 mol/L formaldehyde in 0.1 M phosphate-buffered saline, pH 7.2). The tissues were then embedded in Paraplast Plus blocks (Sigma-Aldrich Co., St. Louis, MO, USA) for subsequent morphological and immunohistochemical analyses.

2.6. Lipid Profile Measurement

Plasma concentrations of triglycerides (TG) (K-117), total cholesterol (TC) (K-083), and high-density lipoprotein (HDL) (K-071) were determined by colorimetric assays using commercial kits, according to the manufacturer's instructions (Bioclin, Belo Horizonte, Minas Gerais, Brazil). Levels of very low-density lipoprotein (VLDL) and low-density lipoprotein (LDL) were calculated based on previously established methods [23].

2.7. Morphological Analysis of the Aorta and Assessment of Collagen Content

The aorta samples previously fixed in formalin (1.27 mol/l formaldehyde, 0.1 M phosphate-buffered saline, pH 7.2), and embedded in Paraplast Plus (Sigma-Aldrich Co., St Louis, MO, USA) blocks were sectioned with 5 μm and stained with hematoxylin-eosin to assess morphological parameters, including lumen diameter, media thickness, media-to-lumen ratio (M/L), circumferential wall tension (CWT) and tensile stress (TS). To evaluate fibrosis, aorta sections of 5 μm were stained with picrosirius red for collagen visualization. Histological images were captured from selected quadrants of the aorta, ensuring at least 8 representative fields per animal, with samples from 5 to 6 animals per group. Images were saved in JPG format, 36-bit color, at a resolution of 1360 × 1024 pixels. Immunostaining was also performed

to determine the type of collagen (I and III) deposited and to quantify fibrosis. All slides were analyzed in a blinded manner, with ten images captured per slide using an optical microscope (Olympus, Tokyo, Japan). Quantitative analysis of aortic parameters was carried out using Image-Pro Plus software (version 7, Media Cybernetics, Silver Spring, MD, USA).

2.8. Immunohistochemistry

Aorta and PVAT sections (5 μm), previously embedded in Paraplast Plus, were deparaffinized, rehydrated, and then incubated with 0.3% hydrogen peroxide for 15 minutes to inhibit endogenous peroxidase activity. Tissue sections were incubated overnight at 4˚C in a humidified chamber with the primary antibody diluted 1:100 in phosphate-buffered saline (PBS). Signal amplification was carried out using a biotin-streptavidin complex system (PK-8800 Vectastain Universal Quick Kit), and positive immunoreactivity was visualized using 3,3'-diaminobenzidine tetrachloride (DAB; K3466, Dako Cytomation, Glostrup, Denmark). The antibodies used in this procedure included those targeting collagen type I and III, AT1 and AT2 receptors, MMP-2, NADPH oxidase 4 (NOX4), peNOS, monocyte chemoattractant protein 1 (MCP-1), Interleukin 6 (IL-6), tumor necrosis factor-alpha (TNF-α) (Santa Cruz Biotechnology, CA, USA), transforming growth factor-beta (TGF-β) (Applied Biological Materials Inc., Canada), eNOS (Novus Biologicals LLC, CO, USA), and 8-isoprostane immunostaining (Oxford Biomedical Research, Inc., MI, USA). The quantification of the number of nuclei/area (1 square micrometer) was performed using the STEPanizer 1 Program (S.A. Tschanz), with four photos/animal (n = 5). The images (TIFF format, 36-bit color, 1360 × 1024 pixels) of each slide were obtained with an Olympus BX40 fluorescence microscope attached to an Olympus DP71 camera (Olympus, Tokyo, Japan). The quantification was performed using ImageJ 1.53 version (National Institutes of Health, MD, USA) by the color deconvolution plug-in, which separates the DAB color spectrum.

2.9. Western Blotting

Protein expression of MMP-2 (1:500), along with key components of the RAS-Renin (1:500), ACE (1:1000), AT1 receptor (1:1000), AT2 receptor (1:500), ACE-2 (1:1000), and β-actin (1:500) (Santa Cruz Biotechnology Inc., CA, USA) was assessed in homogenized aorta samples. Tissues were homogenized in cold lysis buffer (50 mM Tris, pH 7.4, 150 mM NaCl, 0.1% SDS, 5 mM EDTA, 50 mM NaF, and 1% Triton X-100) containing Complete Protease Inhibitor Cocktail Tablets (Roche, Basel, Switzerland) using an Ultra-Turrax homogenizer (IKA Werke GmbH & Co. KG, Staufen, Germany). The total protein content was determined by the BCA protein assay kit (ThermoScientific Inc., Barrington, IL, E). Samples (20 μg total protein) were electrophoresed in 10% tris-glycine sodium dodecyl sulfate-polyacrylamide gels. Proteins were transferred to polyvinylidene fluoride membranes (Hybond ECL; Amersham Pharmacia Biotech, London, UK). The blots were blocked with 5% bovine albumin (Sigma-Aldrich Co., St. Louis, MO, USA) in T-TBS (0.02 M

Tris/0.15 M NaCl, pH 7.5, containing 0.1% Tween 20) at room temperature for 1 h and incubated with primary antibodies (1:1000 concentration) overnight at 4˚C. After washing with T-TBS, blots were incubated with corresponding secondary conjugated antibodies at 1:1000 concentration for 1 h. Antibodies were purchased from Santa Cruz Biotechnology Inc. (Santa Cruz, CA). We also incubated all membranes with the β-actin antibody to avoid possible protein loading and/or transfer inconsistency. Blots were developed with an enhanced luminescence (Amersham ECL Prime Western Blotting, GE Healthcare, UK). The signals were visualized by ChemiDoc XRS+ system (Bio-Rad, Hercules, CA, USA) and analyzed using Adobe Photoshop Elements 11, version 11.0 (Adobe Systems Incorporated). The results were expressed as arbitrary units.

2.10. Statistical Analysis

The data are presented as the mean and standard error of the mean. Differences among groups were analyzed by one-way and two-way analysis of variance (ANOVA) and followed by the post-hoc test of Tukey, considering a confidence interval of 95% ($p < 0.05$). Statistical analysis was made using GraphPad Prism version 8.0 (GraphPad Software, San Diego, USA).

3. Results

3.1. Effects of ASE on Body Weight, Blood Glucose, and Lipid Profile

The body weight of the animals from the three groups was the same at the beginning of the study (Table 1). After 12 weeks, the increase in the body weight induced by the HF diet was prevented by treatment with ASE ($p \leq 0.0001$; n = 15 for each group).

Table 1. Effects of ASE on body weight, glycemia, lipid profile, and adipose tissue in obese mice.

	Control	HF	HF + ASE
Initial body weight (g)	19.7 ± 0.5	19.8 ± 0.3	19.2 ± 0.3
Final body weight (g)	28.9 ± 0.6	41.2 ± 1.2*	30.6 ± 0.8^{+}
Initial glucose (mg/dL)	148.1 ± 3.8	149.3 ± 7.1	157.1 ± 9.4
Final glucose (mg/dL)	138.7 ± 1.8	195.7 ± 4.9*	148.7 ± 4.4^{+}
Plasma			
Cholesterol (mg/dL)	83.3 ± 1.32	161.2 ± 1.7*	115.4 ± 1.2^{+}
Triglycerides (mg/dL)	68.7 ± 3.2	85.2 ± 2.8	54.1 ± 3.6^{+}
LDL (mg/dL)	22.6 ± 2.7	98.7 ± 3.8*	21.6 ± 2.9^{+}
VLDL (mg/dL)	14.2 ± 3.1	17.5 ± 2.5	10.8 ± 3.7^{+}
HDL (mg/dL)	56.4 ± 2.9	48.1 ± 2.7	81.9 ± 2.8^{+}

Values are presented as means ± SEM, n = 15 for all groups for initial body weight, final body weight, initial glucose, and final glucose; n = 10 for total cholesterol, triglycerides, LDL-C, and VLDL-C. *Significantly different from the control ($p \leq 0.05$). $^{+}$Significantly different from the corresponding HF group ($p \leq 0.05$). One-way ANOVA, and post-test of Tukey.

At the beginning of the study, the glycemic levels were similar between the different groups studied (Table 1). At the end of the experimental protocol, the HF group developed hyperglycemia ($p \leq 0.05$), whereas the HF + ASE group remained normoglycemic ($p \leq 0.0001$; $n = 15$ for each group).

The plasma levels of TC and LDL-C were notably higher ($p \leq 0.05$, $n = 10$) in the HF than in the control group at the end of the study period (Table 1). However, the ASE treatment effectively prevented the rise in cholesterol and LDL-C levels in the HF + ASE group compared to the HF group ($p \leq 0.05$), with no significant difference between the HF + ASE and control group. Furthermore, the treatment with ASE led to a reduction in TG and VLDL, and an increase in HDL levels in the HF + ASE group ($p \leq 0.05$) compared with the HF group (Table 1).

3.2. Effect of ASE on Blood Pressure

At the end of the protocol period, the SBP and DBP were increased in the HF group ($p \leq 0.05$) compared with the control group (Figure 1(A) and Figure 1(B)). The treatment with ASE prevented the increase in both SBP and DBP ($p \leq 0.05$) ($n = 15$).

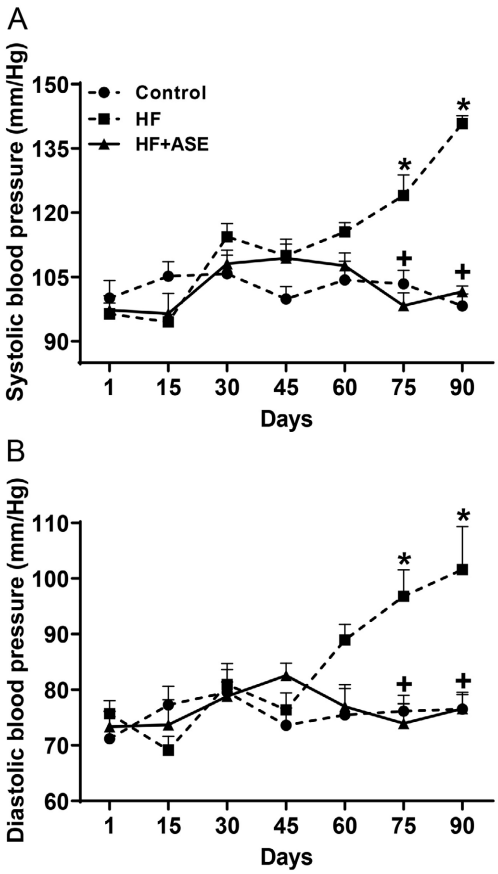

Figure 1. Effect of the treatment with ASE (200 mg/kg/day) on systolic (A) and diastolic (B) blood pressure in mice fed with a high-fat diet. Values are presented as mean ± SEM, $n = 6$ for all groups. *Significantly different ($p < 0.05$) from control group; +Significantly different ($p < 0.05$) from HF group.

3.3. Effect of ASE on Vascular Remodeling

The aorta's lumen diameter was similar between the groups (Figure 2(A) and Figure 2(B); n = 6). Obesity was associated with vascular hypertrophy, as indicated by increased aortic media thickness ($p \leq 0.05$, Figure 2(C) and Figure 2(D)) and increased M/L in the HF group compared to the control group ($p \leq 0.05$, Figure 2(E)). The treatment with ASE prevented both parameters ($p \leq 0.05$, Figures 2(C)-(E)). The CWT was higher in the HF group compared to the control group ($p \leq 0.05$), and this alteration was prevented by the treatment with ASE ($p \leq 0.05$, Figure 2(F)). No difference was observed in TS between groups (Figure 2(G)).

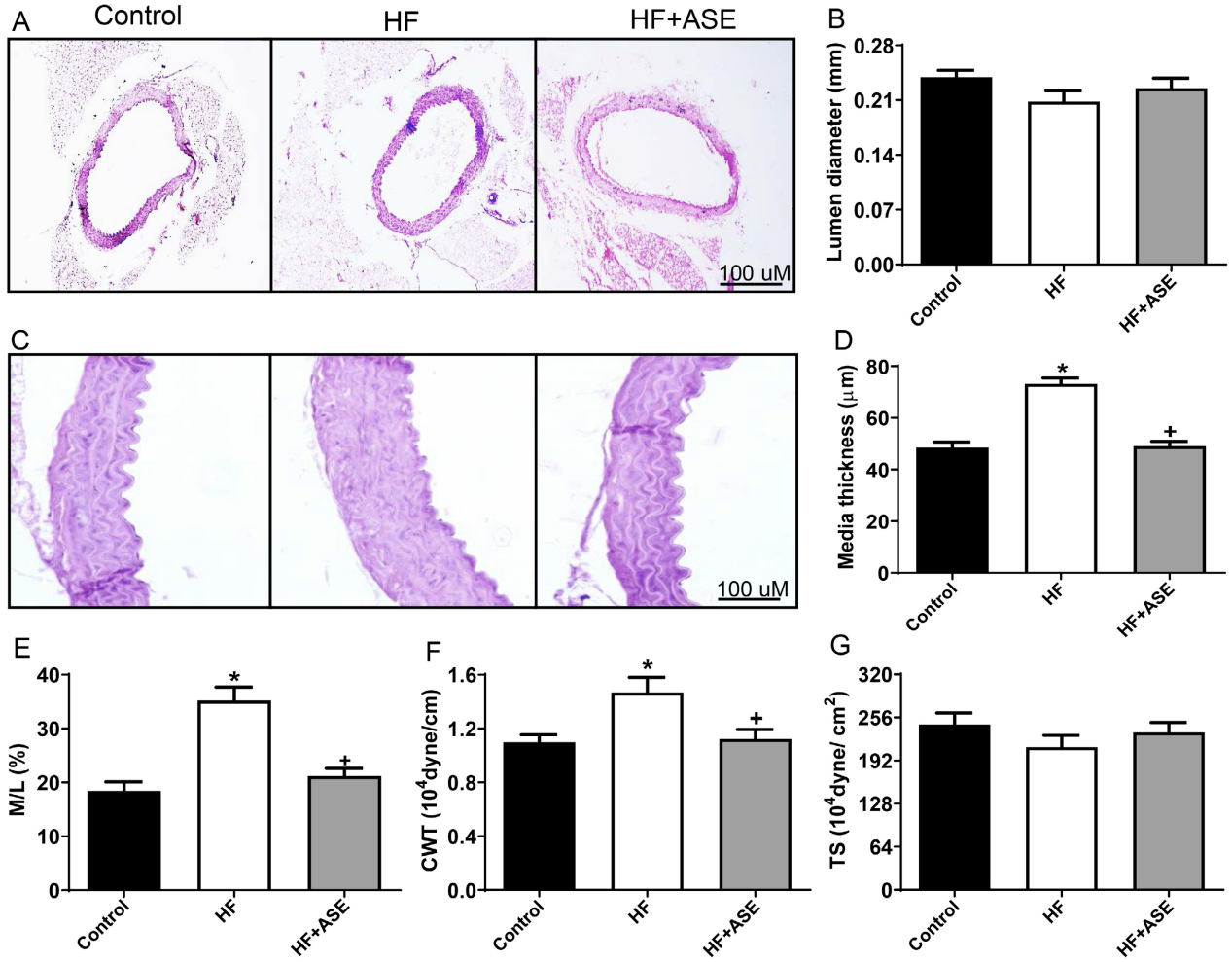

Figure 2. Aorta structure and parameters. Representative sections of aorta ((A) and (C)), stained with hematoxylin and eosin in control, HF and HF + ASE groups (10× and 40× respectively). Effect of ASE on lumen diameter ((A) and (B)), media thickness ((C) and (D)), media-lumen ratio (M/L) (E), circumferential wall tension (CWT) (F) and stress tension (TS) (G) in aorta from HFD-fed mice. Values are presented as mean ± SEM, n = 6 for all groups. *Significantly different ($p < 0.05$) from control group; $^{+}$Significantly different ($p < 0.05$) from HF group.

The HF group showed an increase in aorta total collagen, collagen I, and TGF-β compared to the control group ($p \leq 0.05$, Figures 3(A)-(C), and Figure 3(E)).

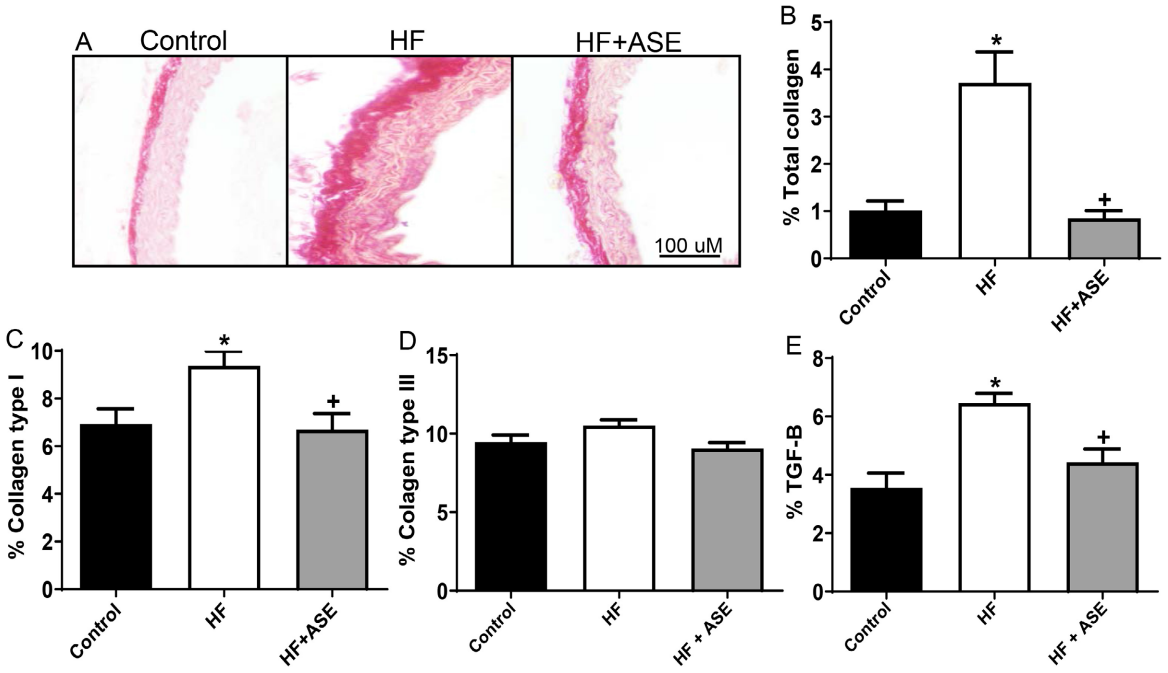

Figure 3. Aorta fibrosis markers. Representative sections of immunostaining and respective % of total collagen ((A) and (B)), collagen type I (C), collagen type III (D), and TGF-β (E) in aorta from control, HF, and HF + ASE groups (40×). Values are presented as mean ± SEM, n = 5 for all groups. *Significantly different ($p < 0.05$) from control group; $^{+}$Significantly different ($p < 0.05$) from HF group.

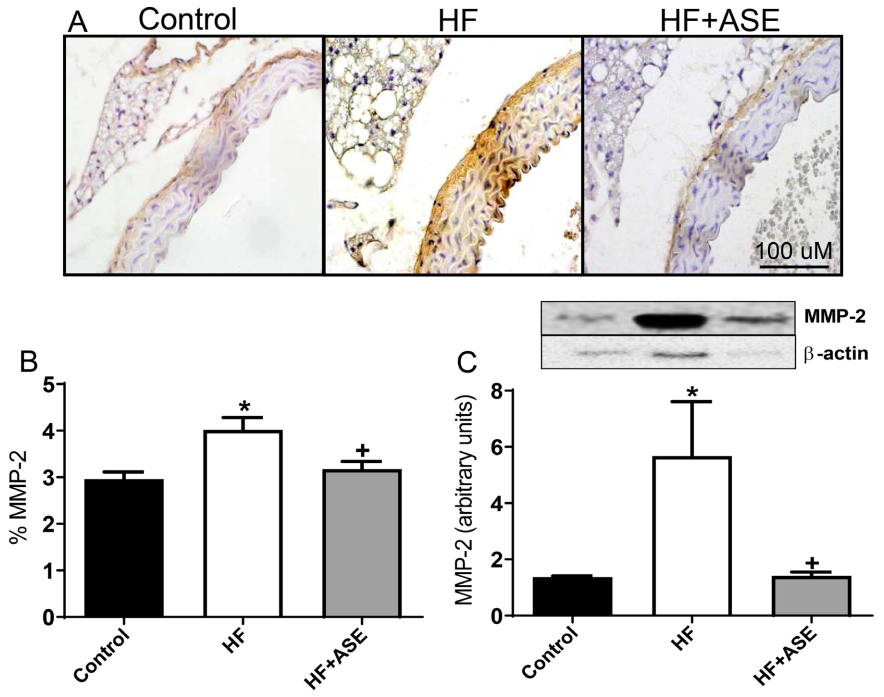

Figure 4. Aorta metalloproteinase analysis. Representative sections of aorta immunostaining, respective % of MMP-2 ((A) and (B)), and Western blotting (C) of MMP-2 in aorta homogenate from control, HF, and HF + ASE groups (40×). The values are presented as mean ± SEM, n = 5 for all groups. *$p < 0.05$ compared to control group; $^{+}p < 0.05$ compared to HF group.

ASE notably impaired this rise, indicating an antifibrotic effect of the extract. Type III collagen was not different between groups ($p \leq 0.05$, Figure 3(D)). The immunostaining and expression of the zinc-dependent endopeptidase MMP-2, implicated in the vascular remodeling of the extracellular matrix, were increased in the aorta of the HF group compared to the control group ($p \leq 0.05$, Figures 4(A)-(C)). The treatment with ASE impaired the up-regulation of this enzyme ($p \leq 0.05$).

3.4. Effect of ASE on Vascular RAS, Oxidative Damage, and Inflammation

We investigated if the extract could modulate local RAS, oxidative damage, and inflammation markers to prevent vascular remodeling. Western blotting analysis

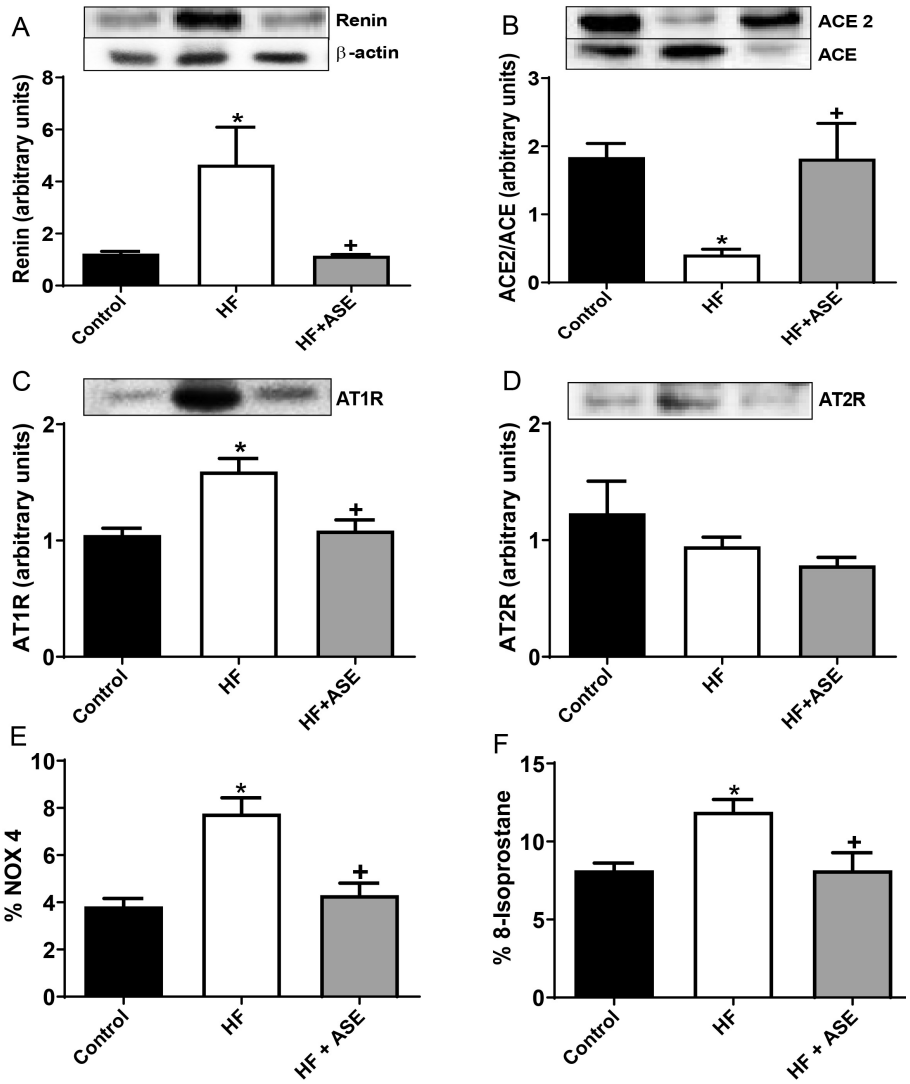

Figure 5. Aorta renin-angiotensin system and oxidative damage markers. Effect of ASE on the RAS components expression, renin (A), ACE2/ACE (B), AT1R (C), AT2R (D), and immunostaining of NOX4 (E) and 8-isoprostane (F) in aorta from control, HF and HF + ASE groups. Values are presented as mean ± SEM, n = 4 for all groups. *Significantly different ($p < 0.05$) from control group; +Significantly different ($p < 0.05$) from HF group.

showed an increase in renin and AT1R protein levels compared to the control group ($p \leq 0.05$, Figure 5(A) and Figure 5(C), n = 4). These increases were prevented by the treatment with ASE, with the treated group showing levels of renin and AT1R proteins similar to the control group ($p \leq 0.05$, Figure 5(A) and Figure 5(C)). This evidence indicates that the HF diet administration activates the principal RAS axis in the aorta in this animal model, which ASE modulates. AT2R protein levels showed no statistical differences between the control and HF groups (Figure 5(D)). The ACE2/ACE ratio was notably decreased in the HF group compared to the control group and prevented by the treatment with ASE ($p \leq 0.05$, Figure 5(B)), indicating that ASE probably activates the alternative RAS axis.

The main enzyme that produces anion superoxide in vessels, NOX4, and the oxidative marker, 8-isoprostane, were increased in the HF group compared to the control group, and the treatment with ASE impaired those increased levels ($p \leq 0.05$, Figure 5(E) and Figure 5(F)).

IL-6, TNF-α and MCP-1 immunostaining showed an increase in all three inflammatory markers in the HF group compared to the control group ($p \leq 0.05$, Figures 6(A)-(C)). The treatment with ASE showed lower levels of the three cytokines than the HF group ($p \leq 0.05$), having similar levels to the control group, proving an anti-inflammatory effect of ASE in the aorta of mice submitted to the HF diet.

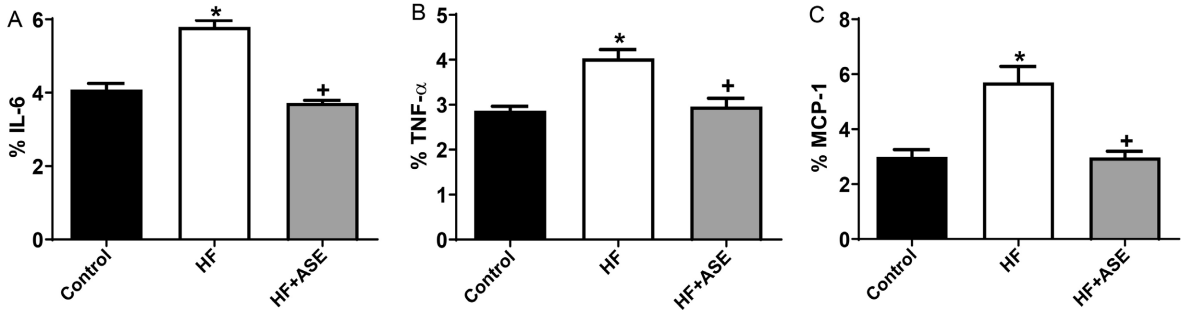

Figure 6. Aorta pro-inflammatory markers. Immunostaining (%) of IL-6 (A), TNF-α (B), and MCP-1 (C) in aorta from control, HF, and HF + ASE groups. Values are presented as mean ± SEM, n = 5 for all groups. *Significantly different ($p < 0.05$) from control group; +Significantly different ($p < 0.05$) from HF group.

3.5. Effect of ASE on Perivascular Adipose Tissue Morphology and Angiotensin II Receptors Content

Histopathological analysis of the PVAT from the CT group showed the characteristic small adipocytes, multiple lipid droplets, and a more significant number of nuclei/area (Figure 7(B) and Figure 7(C)). In contrast, the animals from the HF group showed excessive accumulation of lipids in the adipocytes of the PVAT, resulting in hypertrophic adipocytes (Figure 7(B) and Figure 7(C)), with a lower number of nuclei/area compared to the CT group ($p \leq 0.05$, Figure 7(A), n = 5). Treatment with ASE prevented this change caused by the HF diet, evidenced by an increased density of nuclei per area in the PVAT of the animals in the HF + A group compared with the HF group ($p \leq 0.05$, Figure 7(A)).

AT1R immunostaining in PVAT of HF animals was increased compared to the control group ($p \leq 0.05$, Figure 7(B)). The treatment with ASE showed lower levels of AT1R than the HF group ($p \leq 0.05$, Figure 7(B)), similar to the control group, which indicates modulation of ASE on the angiotensin II receptor in the aorta PVAT of mice submitted to the HF diet. In contrast to the aorta, AT2R levels were decreased in the PVAT of the HF group compared to the control group ($p \leq 0.05$), which was impaired by the treatment with ASE ($p \leq 0.05$, Figure 7(C)), indicating that ASE probably activates the alternative RAS axis in the PVAT.

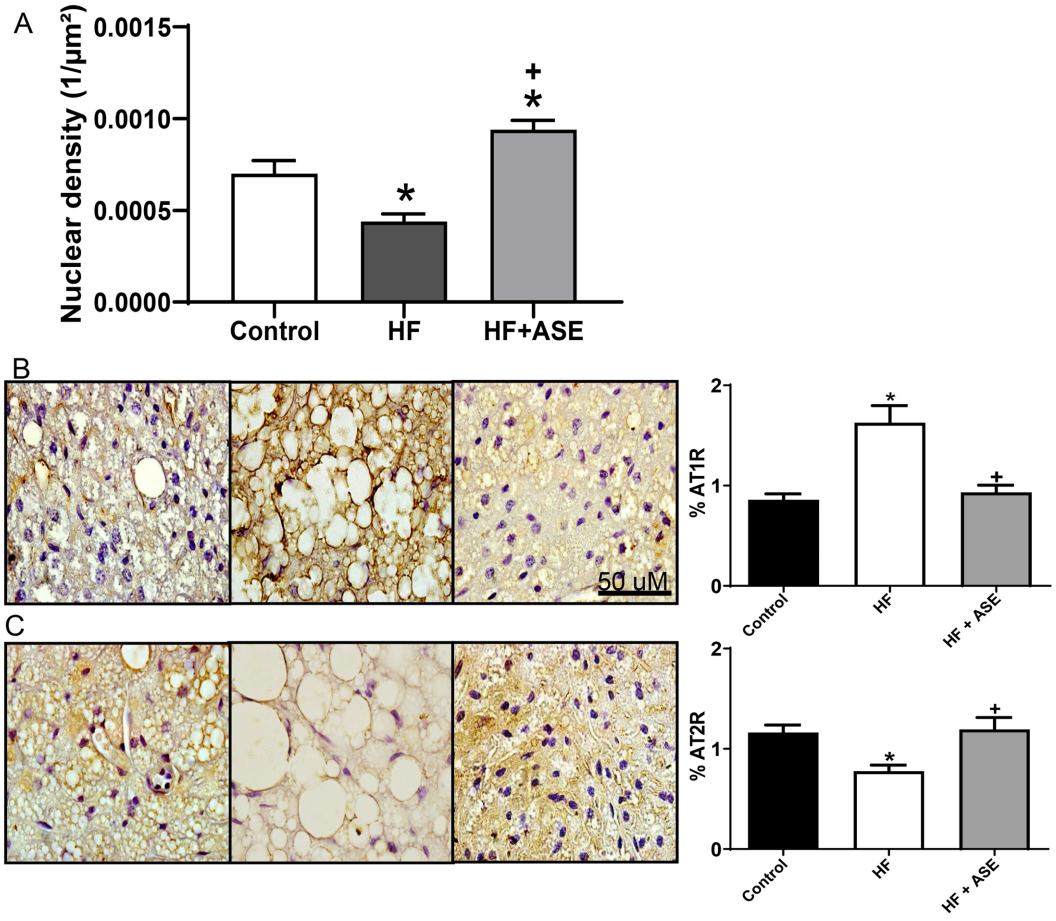

Figure 7. Perivascular adipose tissue structure and angiotensin II markers. Nuclear density (1/µm²) of adipocytes from PVAT (A) in control, HF and HF + ASE groups. Representative sections of immunostaining and respective % of AT1R (B), AT2R (C) in PVAT from control, HF and HF + ASE groups (100×). Values are presented as mean ± SEM, n = 5 for all groups. *Significantly different ($p < 0.05$) from control group; +Significantly different ($p < 0.05$) from HF group.

3.6. Effect of ASE on Perivascular Adipose Tissue Oxidative Damage, eNOS Content, and Inflammation

As observed in the aorta, NOX4 and 8-isoprostane were increased in the HF group compared to the control group, and the treatment with ASE impaired those increased levels ($p \leq 0.05$, Figure 8(A) and Figure 8(B), respectively, n = 5). In contrast, both PVAT eNOS and peNOS were decreased in the HF group, and ASE

treatment brought them to control levels ($p \leq 0.05$, Figure 8(C) and Figure 8(D), respectively).

The inflammatory markers IL-6, TNF-α, and MCP-1 were increased in the PVAT of the HF group compared to the control group ($p \leq 0.05$, Figures 8(E)-(G), n = 5). The treatment with ASE showed lower levels of the three cytokines than the HF group ($p \leq 0.05$), having similar levels to the control group, which aligns with the aorta results.

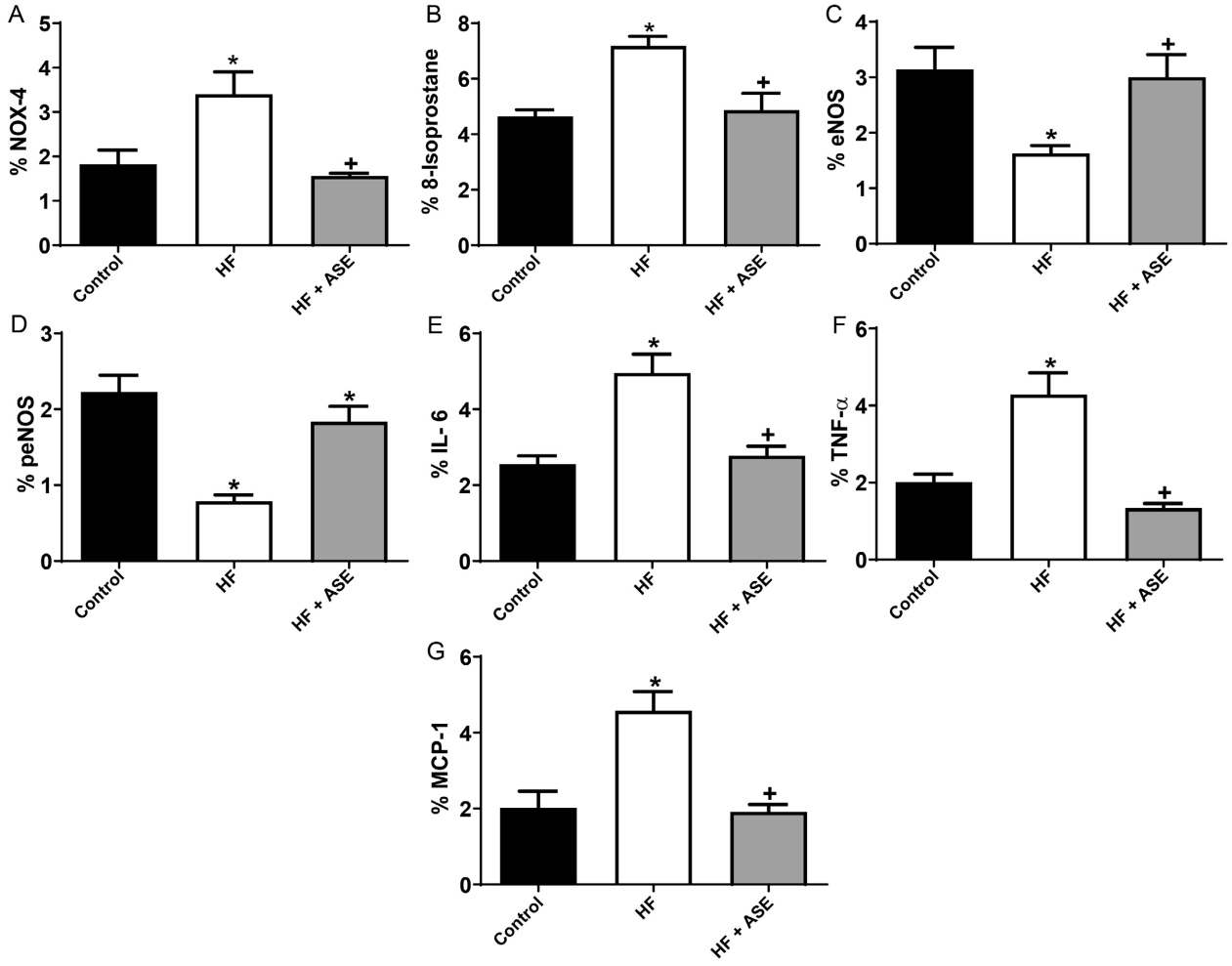

Figure 8. Perivascular adipose tissue oxidative damage, eNOS and pro-inflammatory markers. Immunostaining (%) of NOX-4 (A), 8-isoprostane (B), eNOS and peNOS ((C) and (D)), IL-6 (E), TNF-α (F) and MCP-1 (G) in PVAT from control, HF and HF + ASE groups. Values are presented as mean ± SEM, n = 5 for all groups. *Significantly different ($p < 0.05$) from control group; $^{+}$Significantly different ($p < 0.05$) from HF group.

4. Discussion

Obesity is known to contribute to the onset and progression of both hypertension and insulin resistance, leading to an increase in morbidity and mortality rates [24]. In previous studies conducted by our group, ASE was shown to effectively prevent weight gain, hyperglycemia, dyslipidemia, hypertension, and hepatic steatosis in animals fed a HFD [16] [17] [22] [25]. The notable effectiveness of ASE in miti-

gating obesity-related comorbidities highlights its potential as a promising strategy for managing obesity and its associated health complications.

Vascular remodeling—primarily marked by media thickening and increased arterial stiffness—is a dynamic adaptive process triggered by mechanical and hemodynamic stimuli. It aims to restore wall tension and normalize wall stress in response to various pathological conditions, thereby helping to preserve adequate blood flow [26]. In the setting of obesity, structural and functional alterations in the vasculature progressively lead to increased arterial stiffness [26] [27], which contributes to elevated peripheral vascular resistance and, consequently, higher blood pressure [28]. In this study, obese animals exhibited vascular hypertrophy, evidenced by increased media thickness, consistent with previous findings [29]. This was accompanied by a rise in the media-to-lumen ratio and circumferential wall tension (CWT), both of which are key factors in regulating vascular wall remodeling [30] and were associated with the development of hypertension. Consistent with previous findings, ASE prevented hypertension [25], partly explained by its endothelium-dependent vasodilatory effect, mediated by activation of the NO-cGMP pathway [13]. In this study, ASE treatment effectively prevented the rise in media thickness, media-to-lumen ratio, and CWT, indicating its potential therapeutic role in counteracting vascular remodeling and hypertension linked to obesity. The beneficial effects of ASE on vascular remodeling and obesity may be attributed to its phenolic compounds. Recent studies have shown that oligomeric proanthocyanidins—flavanols found in ASE—can improve lipid profiles in the serum and liver, reduce fat accumulation, and offer protection against cardiovascular remodeling [31] [32]. *In vivo* studies have shown that polymeric proanthocyanidins possess vascular protective properties, such as enhancing endothelial function, preventing LDL oxidation, and modulating both blood pressure and vascular inflammation [33] [34]. These flavanols have been shown to modulate lipid metabolism and fat accumulation, which are key contributors to vascular pathology. The reduction in systemic lipid burden and adiposity may, in turn, alleviate endothelial stress and inflammatory signaling, thereby reinforcing the vascular protective effects observed in our model.

A key feature of vascular remodeling is the reorganization of the ECM, a process largely driven by matrix metalloproteinases (MMPs), which degrade ECM components and alter the balance of collagen and elastin, contributing to arterial stiffness [26] [35]. Vascular fibrosis, commonly observed in obesity-related vascular changes, is characterized by the accumulation of collagen type I, the predominant collagen at the vascular level, and is closely linked to vascular hypertrophy [26] [31] [35]. Evidence also indicates that the profibrotic cytokine TGF-β plays a significant role in promoting vascular fibrosis in the context of obesity [36]. Our findings demonstrate that the coexistence of hypertension and obesity exacerbates vascular fibrosis, as indicated by elevated MMP-2 expression and deposition, increased total and type I collagen content, and higher TGF-β levels in the HFD group. ASE treatment effectively prevented these changes, suggesting a protective effect of the

extract against obesity-induced vascular fibrosis, an essential feature of vascular remodeling.

The hemodynamic and vascular structural alterations observed in individuals with excess weight may be linked to dysregulation of the vascular RAS, as indicated by elevated levels of angiotensin II (Ang II), a potent vasoconstrictor and key effector of the RAS [9]. It contributes to vascular muscle cell proliferation, hypertrophy, and fibrosis, which leads to arterial stiffness [9] [37]-[39]. Notably, RAS upregulation also occurs within the PVAT, which influences vascular tone and structure through both contact-dependent and paracrine mechanisms. These regulatory functions are disrupted in obesity, as demonstrated in both mice and humans [24] [40]-[42]. In individuals with obesity, activation of the Ang II type 1 receptor (AT1R) contributes to elevated oxidative stress and reduced nitric oxide (NO) availability by inhibiting eNOS activity in both vascular endothelial cells [43] and dysfunctional PVAT [40]. Additionally, PVAT dysfunction in obesity leads to eNOS uncoupling and further decreases NO bioavailability, partly due to a deficiency in L-arginine [44]. Our results reveal a positive interaction between vascular and PVAT remodeling, RAS components expression, and oxidative stress markers (NOX4 and 8-isoprostane), along with reduced deposition of eNOS and peNOS in PVAT. These findings are possibly due to Ang II-induced oxidative stress, contributing to vascular remodeling and dysfunction [40].

Previous research from our group demonstrated that ASE can regulate the local RAS in the liver of HFD-fed mice [16] and exhibits antioxidant properties in experimental models of hypertension, diabetes, and obesity [14] [17] [45]. Our current findings reveal that ASE inhibits the upregulation of key RAS components, specifically renin and AT1 receptor in the aorta, and AT1 receptor in PVAT, which are involved in driving proliferative, pro-inflammatory, and fibrotic processes mediated by AT1R. These results indicate that ASE exerts critical regulatory effects on the RAS within both tissues, contributing to the maintenance of vascular homeostasis and blood pressure control [46] [47]. At the same time, the up-regulation of ACE2/ACE expression in the aorta, along with enhanced AT2R deposition in PVAT, suggests that ASE activates the alternative RAS axis components within both the vessel wall and PVAT, counterbalancing AT1R-mediated actions. Previous findings in visceral white adipose tissue have demonstrated that the same extract composed of proanthocyanidins, catechins, and epicatechin reduced the oxidative stress and lowered the expression of renin and AT1, but did not affect the alternative RAS axis components [17]. However, the present results, corroborate our previous findings in liver of the same experimental model, in which we observed an up-regulation of alternative RAS axis, indicating a possible tissue-specific enhancement of protective RAS pathways in the metabolic and vascular context, These findings suggest that while ASE exerts broad inhibitory effects on the classical RAS axis across multiple tissues, its ability to modulate the alternative RAS may vary in a tissue-dependent manner, potentially reflecting distinct physiological roles in metabolic versus vascular tissues. Overall, our findings suggest that ASE promotes

protection against vascular and PVAT remodeling by regulating RAS, reducing oxidative stress and enhancing NO bioavailability in HFD-fed mice, which may contribute to preventing obesity-related vascular structural changes and hypertension. Given the key role of PVAT in controlling vascular tone and structure [24] [40], our findings imply that ASE could exert its beneficial effects both directly on the vascular wall and indirectly through paracrine signaling from the PVAT, contributing to improved vascular remodeling.

Chronic low-grade inflammation is increasingly acknowledged as a key factor in the development of arterial stiffness and vascular remodeling linked to obesity [7]. PVAT contributes significantly to this inflammatory milieu by releasing elevated levels of pro-inflammatory cytokines and adipokines such as MCP-1, TNF-*α*, IL-6, Ang II, leptin, visfatin, and resistin within the local vascular environment. Conversely, levels of anti-inflammatory adipocytokines, especially adiponectin, are diminished in dysfunctional PVAT [48]. As a result, inflammation within obese PVAT exacerbates the generation of reactive oxygen species (ROS), notably superoxide (O_2^-) and hydrogen peroxide (H_2O_2) [49]. These findings emphasize the connection between RAS activation, oxidative stress and inflammation in PVAT and adjacent vasculature, particularly in the progression of vascular dysfunction [50].

Our results demonstrated a similar pro-inflammatory profile in both aorta and PVAT, evidenced by increased IL-6, TNF-*α*, and MCP-1 deposition in these tissues. This pro-inflammatory condition was prevented by ASE, reinforcing the potent anti-inflammatory effects of ASE previously reported in other tissues and animal models [15] [45]. The antioxidant and anti-inflammatory properties of proanthocyanidins, the main flavanol component in ASE, have also been observed in extracts from other plants like *Uncaria tomentosa* L., *Annona Crassiflora* Mart, *and Gaultheria procumbens* L. [32]. Additionally, epicatechins, another flavanol found in ASE, are known for their antioxidant and anti-inflammatory activities. They neutralize ROS and enhance endogenous defense systems by activating the Nrf2 signaling pathway [51] [52]. While epicatechins have been reported to activate the Nrf2 signaling pathway, we did not directly assess Nrf2 activation in this study. Future research will be necessary to determine whether the observed effects are mediated, at least in part, via Nrf2-dependent mechanisms. This study provides the first evidence of ASE's antioxidant and anti-inflammatory effects in both the aorta and PVAT of obese mice. These findings suggest that ASE may interrupt the pro-inflammatory crosstalk between these tissues, thereby offering protection against vascular remodeling associated with obesity. Taken together, our findings suggest that ASE prevents vascular and PVAT remodeling through a multifactorial mechanism involving modulation of the RAS, attenuation of oxidative stress, and suppression of inflammation. Among these, the RAS may act as a central node, as its dysregulation is known to trigger both oxidative and inflammatory cascades. Thus, it is plausible that ASE's impact on this system serves as a primary driver that orchestrates downstream protective effects. Further research, including mechanistic

investigations and bioavailability studies, is necessary to better define the therapeutic potential of the polyphenols found in açaí seed extract.

5. Conclusion

In conclusion, ASE treatment in HFD-fed mice effectively prevented aortic hypertrophy, fibrosis, and PVAT hypertrophy, key features of vascular remodeling associated with an anti-hypertensive effect. The observed modulation of the RAS, oxidative stress, and inflammation in both the aortic wall and PVAT suggests an interaction between these mechanisms that contributes to ASE's protective effects. These findings highlight ASE's potential as a promising therapeutic approach for managing obesity-related vascular diseases.

Funding

This work was supported by the National Council of Scientific and Technological Development/CNPq (grant number 304381/2021-7) and the Rio de Janeiro State Research Agency/FAPERJ (grant numbers E-26/200.931/2021, E-26/211.287/2021).

Acknowledgements

The authors thank the Higher Education Personnel Improvement Coordination/CAPES for postgraduate scholarships.

Conflicts of Interest

The authors declare no conflicts of interest regarding the publication of this paper.

References

[1] Flores-Ortiz, R., Malta, D.C. and Velasquez-Melendez, G. (2019) Adult Body Weight Trends in 27 Urban Populations of Brazil from 2006 to 2016: A Population-Based Study. *PLOS ONE*, **14**, e0213254. https://doi.org/10.1371/journal.pone.0213254

[2] Mahmood, S.S., Levy, D., Vasan, R.S. and Wang, T.J. (2014) The Framingham Heart Study and the Epidemiology of Cardiovascular Disease: A Historical Perspective. *The Lancet*, **383**, 999-1008. https://doi.org/10.1016/s0140-6736(13)61752-3

[3] Fuster, J.J., Ouchi, N., Gokce, N. and Walsh, K. (2016) Obesity-Induced Changes in Adipose Tissue Microenvironment and Their Impact on Cardiovascular Disease. *Circulation Research*, **118**, 1786-1807. https://doi.org/10.1161/circresaha.115.306885

[4] Townsend, R.R., Wilkinson, I.B., Schiffrin, E.L., Avolio, A.P., Chirinos, J.A., Cockcroft, J.R., *et al.* (2015) Recommendations for Improving and Standardizing Vascular Research on Arterial Stiffness. *Hypertension*, **66**, 698-722. https://doi.org/10.1161/hyp.0000000000000033

[5] Cote, A.T., Phillips, A.A., Harris, K.C., Sandor, G.G.S., Panagiotopoulos, C. and Devlin, A.M. (2015) Obesity and Arterial Stiffness in Children: Systematic Review and Meta-Analysis. *Arteriosclerosis, Thrombosis, and Vascular Biology*, **35**, 1038-1044. https://doi.org/10.1161/atvbaha.114.305062

[6] Weberruß, H., Pirzer, R., Böhm, B., Dalla Pozza, R., Netz, H. and Oberhoffer, R. (2015) Intima-Media Thickness and Arterial Function in Obese and Non-Obese Children. *BMC Obesity*, **3**, Article No. 2. https://doi.org/10.1186/s40608-016-0081-9

[7] Aroor, A., McKarns, S., Nistala, R., DeMarco, V., Gardner, M., Garcia-Touza, M., Whaley-Connell, A. and Sowers, J.R. (2013) DPP-4 Inhibitors as Therapeutic Modulators of Immune Cell Function and Associated Cardiovascular and Renal Insulin Resistance in Obesity and Diabetes. *Cardiorenal Medicine*, **3**, 48-56.

[8] Gao, J., Xie, Q., Wei, T., Huang, C., Zhou, W. and Shen, W. (2019) Nebivolol Improves Obesity-Induced Vascular Remodeling by Suppressing NLRP3 Activation. *Journal of Cardiovascular Pharmacology*, **73**, 326-333. https://doi.org/10.1097/fjc.0000000000000667

[9] Aroor, A.R., Jia, G. and Sowers, J.R. (2018) Cellular Mechanisms Underlying Obesity-Induced Arterial Stiffness. *American Journal of Physiology-Regulatory, Integrative and Comparative Physiology*, **314**, R387-R398. https://doi.org/10.1152/ajpregu.00235.2016

[10] Jia, G., Aroor, A.R., DeMarco, V.G., Martinez-Lemus, L.A., Meininger, G.A. and Sowers, J.R. (2015) Vascular Stiffness in Insulin Resistance and Obesity. *Frontiers in Physiology*, **6**, Article 301. https://doi.org/10.3389/fphys.2015.00231

[11] Koskinas, K.C., Van Craenenbroeck, E.M., Antoniades, C., Blüher, M., Gorter, T.M., Hanssen, H., *et al.* (2024) Obesity and Cardiovascular Disease: An ESC Clinical Consensus Statement. *European Heart Journal*, **45**, 4063-4098. https://doi.org/10.1093/eurheartj/ehae508

[12] Rocha, A.P.M., Carvalho, L.C.R.M., Sousa, M.A.V., Madeira, S.V.F., Sousa, P.J.C., Tano, T., *et al.* (2007) Endothelium-Dependent Vasodilator Effect of *Euterpe oleracea* Mart. (Açaí) Extracts in Mesenteric Vascular Bed of the Rat. *Vascular Pharmacology*, **46**, 97-104. https://doi.org/10.1016/j.vph.2006.08.411

[13] Rocha, A.P.M., Resende, A.C., Souza, M.A.V., Carvalho, L.C.R.M., Sousa, P.J.C., Tano, T., *et al.* (2008) Antihypertensive Effects and Antioxidant Action of a Hydro-Alcoholic Extract Obtained from Fruits of *Euterpe oleracea* Mart. (Acai). *Journal of Pharmacology and Toxicology*, **3**, 435-448. https://doi.org/10.3923/jpt.2008.435.448

[14] da Costa, C.A., de Oliveira, P.R.B., de Bem, G.F., de Cavalho, L.C.R.M., Ognibene, D.T., da Silva, A.F.E., *et al.* (2012) *Euterpe oleracea* Mart.-Derived Polyphenols Prevent Endothelial Dysfunction and Vascular Structural Changes in Renovascular Hypertensive Rats: Role of Oxidative Stress. *Naunyn-Schmiedeberg's Archives of Pharmacology*, **385**, 1199-1209. https://doi.org/10.1007/s00210-012-0798-z

[15] de Moura, R.S., Ferreira, T.S., Lopes, A.A., Pires, K.M.P., Nesi, R.T., Resende, A.C., *et al.* (2012) Effects of *Euterpe oleracea* Mart. (Açaí) Extract in Acute Lung Inflammation Induced by Cigarette Smoke in the Mouse. *Phytomedicine*, **19**, 262-269. https://doi.org/10.1016/j.phymed.2011.11.004

[16] Romão, M.H., de Bem, G.F., Santos, I.B., de Andrade Soares, R., Ognibene, D.T., de Moura, R.S., *et al.* (2020) Açaí (*Euterpe oleracea* Mart.) Seed Extract Protects against Hepatic Steatosis and Fibrosis in High-Fat Diet-Fed Mice: Role of Local Renin-Angiotensin System, Oxidative Stress and Inflammation. *Journal of Functional Foods*, **65**, Article ID: 103726. https://doi.org/10.1016/j.jff.2019.103726

[17] Santos, I.B., de Bem, G.F., da Costa, C.A., de Carvalho, L.C.R.M., de Medeiros, A.F., Silva, D.L.B., *et al.* (2020) Açaí Seed Extract Prevents the Renin-Angiotensin System Activation, Oxidative Stress and Inflammation in White Adipose Tissue of High-Fat Diet-Fed Mice. *Nutrition Research*, **79**, 35-49. https://doi.org/10.1016/j.nutres.2020.05.006

[18] Carmo, L.S., Burdmann, E.A., Fessel, M.R., Almeida, Y.E., Pescatore, L.A., Farias-Silva, E., *et al.* (2019) Expansive Vascular Remodeling and Increased Vascular Calcification Response to Cholecalciferol in a Murine Model of Obesity and Insulin Resistance.

Arteriosclerosis, Thrombosis, and Vascular Biology, **39**, 200-211. https://doi.org/10.1161/atvbaha.118.311880

[19] Xia, N. and Li, H. (2016) The Role of Perivascular Adipose Tissue in Obesity-Induced Vascular Dysfunction. *British Journal of Pharmacology*, **174**, 3425-3442. https://doi.org/10.1111/bph.13650

[20] Agabiti-Rosei, C., Paini, A., De Ciuceis, C., Withers, S., Greenstein, A., Heagerty, A.M., *et al.* (2018) Modulation of Vascular Reactivity by Perivascular Adipose Tissue (PVAT). *Current Hypertension Reports*, **20**, Article No. 44. https://doi.org/10.1007/s11906-018-0835-5

[21] Aroor, A.R., DeMarco, V.G., Jia, G., Sun, Z., Nistala, R., Meininger, G.A., *et al.* (2013) The Role of Tissue Renin-Angiotensin-Aldosterone System in the Development of Endothelial Dysfunction and Arterial Stiffness. *Frontiers in Endocrinology*, **4**, Article 161. https://doi.org/10.3389/fendo.2013.00161

[22] de Oliveira, P.R.B., da Costa, C.A., de Bem, G.F., Cordeiro, V.S.C., Santos, I.B., de Carvalho, L.C.R.M., *et al.* (2015) *Euterpe oleracea* Mart.-Derived Polyphenols Protect Mice from Diet-Induced Obesity and Fatty Liver by Regulating Hepatic Lipogenesis and Cholesterol Excretion. *PLOS ONE*, **10**, e0143721. https://doi.org/10.1371/journal.pone.0143721

[23] de Bem, G.F., Costa, C.A., Santos, I.B., Cristino Cordeiro, V.d.S., de Carvalho, L.C.R.M., de Souza, M.A.V., *et al.* (2018) Antidiabetic Effect of *Euterpe oleracea* Mart. (Açaí) Extract and Exercise Training on High-Fat Diet and Streptozotocin-Induced Diabetic Rats: A Positive Interaction. *PLOS ONE*, **13**, e0199207. https://doi.org/10.1371/journal.pone.0199207

[24] Koenen, M., Hill, M.A., Cohen, P. and Sowers, J.R. (2021) Obesity, Adipose Tissue and Vascular Dysfunction. *Circulation Research*, **128**, 951-968. https://doi.org/10.1161/circresaha.121.318093

[25] de Oliveira, P.R.B., da Costa, C.A., de Bem, G.F., Marins de Cavalho, L.C.R., de Souza, M.A.V., de Lemos Neto, M., *et al.* (2010) Effects of an Extract Obtained from Fruits of *Euterpe oleracea* Mart. in the Components of Metabolic Syndrome Induced in C57BL/6J Mice Fed a High-Fat Diet. *Journal of Cardiovascular Pharmacology*, **56**, 619-626. https://doi.org/10.1097/fjc.0b013e3181f78da4

[26] Martínez-Martínez, E., Souza-Neto, F., Jiménez-González, S. and Cachofeiro, V. (2021) Oxidative Stress and Vascular Damage in the Context of Obesity: The Hidden Guest. *Antioxidants*, **10**, Article No. 406. https://doi.org/10.3390/antiox10030406

[27] Johnston, E.K. and Abbott, R.D. (2023) Adipose Tissue Paracrine-, Autocrine-, and Matrix-Dependent Signaling during the Development and Progression of Obesity. *Cells*, **12**, Article No. 407. https://doi.org/10.3390/cells12030407

[28] Eikås, J.G., Gerdts, E., Halland, H., Midtbø, H., Cramariuc, D. and Kringeland, E. (2023) Arterial Stiffness in Overweight and Obesity: Association with Sex, Age, and Blood Pressure. *High Blood Pressure & Cardiovascular Prevention*, **30**, 435-443. https://doi.org/10.1007/s40292-023-00593-2

[29] de Moraes Arnoso, B.J., Magliaccio, F.M., de Araújo, C.A., de Andrade Soares, R., Santos, I.B., de Bem, G.F., *et al.* (2022) Açaí Seed Extract (ASE) Rich in Proanthocyanidins Improves Cardiovascular Remodeling by Increasing Antioxidant Response in Obese High-Fat Diet-Fed Mice. *Chemico-Biological Interactions*, **351**, Article ID: 109721. https://doi.org/10.1016/j.cbi.2021.109721

[30] Kassab, G.S. (2006) Biomechanics of the Cardiovascular System: The Aorta as an Illustratory Example. *Journal of The Royal Society Interface*, **3**, 719-740. https://doi.org/10.1098/rsif.2006.0138

[31] Shirwany, N.A. and Zou, M. (2010) Arterial Stiffness: A Brief Review. *Acta Pharmacologica Sinica*, **31**, 1267-1276. https://doi.org/10.1038/aps.2010.123

[32] Nie, F., Liu, L., Cui, J., Zhao, Y., Zhang, D., Zhou, D., *et al.* (2023) Oligomeric Proanthocyanidins: An Updated Review of Their Natural Sources, Synthesis, and Potentials. *Antioxidants*, **12**, Article No. 1004. https://doi.org/10.3390/antiox12051004

[33] Mattioli, R., Francioso, A., Mosca, L. and Silva, P. (2020) Anthocyanins: A Comprehensive Review of Their Chemical Properties and Health Effects on Cardiovascular and Neurodegenerative Diseases. *Molecules*, **25**, Article No. 3809. https://doi.org/10.3390/molecules25173809

[34] Zhao, Y., Wang, L., Huang, Y., Evans, P.C., Little, P.J., Tian, X., *et al.* (2024) Anthocyanins in Vascular Health and Disease: Mechanisms of Action and Therapeutic Potential. *Journal of Cardiovascular Pharmacology*, **84**, 289-302. https://doi.org/10.1097/fjc.0000000000001602

[35] Liu, S., Bae, Y.H., Yu, C., Monslow, J., Hawthorne, E.A., Castagnino, P., *et al.* (2015) Matrix Metalloproteinase-12 Is an Essential Mediator of Acute and Chronic Arterial Stiffening. *Scientific Reports*, **5**, Article No. 17189. https://doi.org/10.1038/srep17189

[36] Frangogiannis, N.G. (2020) Transforming Growth Factor-β in Tissue Fibrosis. *Journal of Experimental Medicine*, **217**, e20190103. https://doi.org/10.1084/jem.20190103

[37] Kim, E.N., Kim, M.Y., Lim, J.H., Kim, Y., Shin, S.J., Park, C.W., *et al.* (2018) The Protective Effect of Resveratrol on Vascular Aging by Modulation of the Renin-Angiotensin System. *Atherosclerosis*, **270**, 123-131. https://doi.org/10.1016/j.atherosclerosis.2018.01.043

[38] Krueger, F., Kappert, K., Foryst-Ludwig, A., Kramer, F., Clemenz, M., Grzesiak, A., *et al.* (2017) At1-Receptor Blockade Attenuates Outward Aortic Remodeling Associated with Diet-Induced Obesity in Mice. *Clinical Science*, **131**, 1989-2005. https://doi.org/10.1042/cs20170131

[39] Corry, D.B., Eslami, P., Yamamoto, K., Nyby, M.D., Makino, H. and Tuck, M.L. (2008) Uric Acid Stimulates Vascular Smooth Muscle Cell Proliferation and Oxidative Stress via the Vascular Renin-Angiotensin System. *Journal of Hypertension*, **26**, 269-275. https://doi.org/10.1097/hjh.0b013e3282f240bf

[40] Cheng, C.K., Ding, H., Jiang, M., Yin, H., Gollasch, M. and Huang, Y. (2023) Perivascular Adipose Tissue: Fine-Tuner of Vascular Redox Status and Inflammation. *Redox Biology*, **62**, Article ID: 102683. https://doi.org/10.1016/j.redox.2023.102683

[41] Gao, Y., Zeng, Z., Teoh, K., Sharma, A.M., Abouzahr, L., Cybulsky, I., *et al.* (2005) Perivascular Adipose Tissue Modulates Vascular Function in the Human Internal Thoracic Artery. *The Journal of Thoracic and Cardiovascular Surgery*, **130**, 1130-1136. https://doi.org/10.1016/j.jtcvs.2005.05.028

[42] Gu, P. and Xu, A. (2013) Interplay between Adipose Tissue and Blood Vessels in Obesity and Vascular Dysfunction. *Reviews in Endocrine and Metabolic Disorders*, **14**, 49-58. https://doi.org/10.1007/s11154-012-9230-8

[43] Ding, J., Yu, M., Jiang, J., Luo, Y., Zhang, Q., Wang, S., *et al.* (2020) Angiotensin II Decreases Endothelial Nitric Oxide Synthase Phosphorylation via AT1R Nox/ROS/PP2A Pathway. *Frontiers in Physiology*, **11**, Article 566410. https://doi.org/10.3389/fphys.2020.566410

[44] Zaborska, K.E., Wareing, M. and Austin, C. (2016) Comparisons between Perivascular Adipose Tissue and the Endothelium in Their Modulation of Vascular Tone. *British Journal of Pharmacology*, **174**, 3388-3397. https://doi.org/10.1111/bph.13648

[45] da Silva Cristino Cordeiro, V., de Bem, G.F., da Costa, C.A., Santos, I.B., de Carvalho,

L.C.R.M., Ognibene, D.T., *et al.* (2017) *Euterpe oleracea* Mart. Seed Extract Protects against Renal Injury in Diabetic and Spontaneously Hypertensive Rats: Role of Inflammation and Oxidative Stress. *European Journal of Nutrition*, **57**, 817-832. https://doi.org/10.1007/s00394-016-1371-1

[46] Poznyak, A.V., Bharadwaj, D., Prasad, G., Grechko, A.V., Sazonova, M.A. and Orekhov, A.N. (2021) Renin-Angiotensin System in Pathogenesis of Atherosclerosis and Treatment of CVD. *International Journal of Molecular Sciences*, **22**, Article No. 6702. https://doi.org/10.3390/ijms22136702

[47] Balakumar, P., Orayj, K.M., Khan, N.A., Shanmugam, K. and Jagadeesh, G. (2024) Impact of the Local Renin-Angiotensin System in Perivascular Adipose Tissue on Vascular Health and Disease. *Cellular Signalling*, **124**, Article ID: 111461. https://doi.org/10.1016/j.cellsig.2024.111461

[48] Chang, L., Garcia-Barrio, M.T. and Chen, Y.E. (2020) Perivascular Adipose Tissue Regulates Vascular Function by Targeting Vascular Smooth Muscle Cells. *Arteriosclerosis, Thrombosis, and Vascular Biology*, **40**, 1094-1109. https://doi.org/10.1161/atvbaha.120.312464

[49] Barp, C.G., Bonaventura, D. and Assreuy, J. (2021) NO, ROS, RAS, and PVAT: More than a Soup of Letters. *Frontiers in Physiology*, **12**, Article 640021. https://doi.org/10.3389/fphys.2021.640021

[50] Stanek, A., Brożyna-Tkaczyk, K. and Myśliński, W. (2021) The Role of Obesity-Induced Perivascular Adipose Tissue (PVAT) Dysfunction in Vascular Homeostasis. *Nutrients*, **13**, Article No. 3843. https://doi.org/10.3390/nu13113843

[51] Jiang, C., Zhuge, X., Li, D., Chen, M., Hu, W. and Xie, L. (2024) Epicatechin-Mediated Modulation of the Nrf2/HO-1 Pathway Alleviates Senile Cerebral Ischemic/Reperfusion Injury. *Food Science & Nutrition*, **12**, 6521-6533. https://doi.org/10.1002/fsn3.4253

[52] Bettaieb, A., Cremonini, E., Kang, H., Kang, J., Haj, F.G. and Oteiza, P.I. (2016) Anti-inflammatory Actions of (−)-Epicatechin in the Adipose Tissue of Obese Mice. *The International Journal of Biochemistry & Cell Biology*, **81**, 383-392. https://doi.org/10.1016/j.biocel.2016.08.044